Wideband Tunable RF Filters for Channel Selection in Crowded Spectral Bands

Sanghoon Park, Ki-Jin Kim, Kwang-Ho Ahn, Hyeon-Woo Lee

***Abstract*—**It is very effective way to utilize a very wide tunable filter in co-existing multi-standards wireless communications environment. Especially, as the long term evolution (LTE) communication era has come, the multi-band coverage is one of the important features required for the RF components. In this paper, we present the frequency conversion technique, and so generate two types of RF filters which are specially designed for the superb tunable ability to support multiple wireless communication standards. With the help of a complex mixing structure, the inherent image signal is suppressed. The RF band-pass filter (BPF) and notch filter achieve 1.8dB and 1.6dB insertion losses and 18 dB and 17 dB attenuations, respectively. The quality factor show greater than 30.

***Keywords*—**RF filters, interference, wideband, tunable, channel selection, complex mixing, balanced mixer.

I. Introduction

WIDEBAND tunable as well as high-quality (Q) RF filter is highly useful in very crowded frequency bands such as co-existing multi-standards wireless communications environment. However, it is very difficult problems in building direct channel selection or notch filters in RF frequency. Surface acoustic wave (SAW) or micro-electro-mechanical systems (MEMS) filters are good candidates for wireless interference suppression applications [1]-[4], but they have well-known size and cost issues. An active circuit technique to synthesize an interference suppression filter has the advantage of straightforward integration [5], [6], but its performance is usually limited in RF applications. The basic concept of the presented filter is back to the well-known N-path filter [7], [8]. The design technique for a wideband high-Q RF filter utilizes the frequency conversion property of the mixer.

Sanghoon Park received the Ph.D. degree from University of California – San Diego, CA 92037, USA. He is with Korea Electronics Technology Institutes, Gyeonggi-do 463-816, Republic of Korea (South) (phone: +82-31-789-7239; fax:+82-31-789-7259; e-mail: parksh@keti.re.kr).

Ki-Jim Kim received the Ph.D. degree from Korea Advanced Institute of Science and Technology, Daejeon-si 305-701, Republic of Korea (South). He is with Korea Electronics Technology Institutes, Gyeonggi-do 463-816, Republic of Korea (South) (e -mail: kijinkim@kaist.ac.kr).

Kwang-Ho Ahn received the Ph.D. degree from Pohang University of Science and Technology, Pohang-si 790-784, Republic of Korea (South). He is with Korea Electronics Technology Institutes, Gyeonggi-do 463-816, Republic of Korea (South) (e-mail: khajoh@keti.re.kr).

Hyeon-Woo Lee received the Ph.D. degree from Korea Advanced Institute of Science and Technology, Daejeon-si 305-701, Republic of Korea (South). He is associate professor in Dankook university, Gyeonggi-do 448-701, Republic of Korea (South) (e -mail: woojaa@dankook.ac.kr).

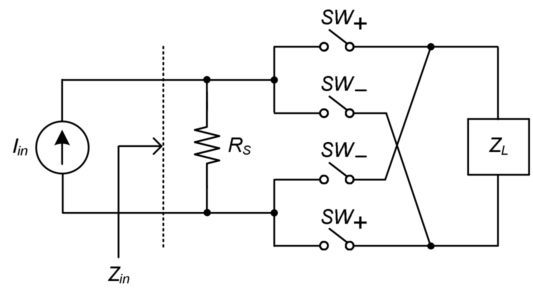

Fig. 1 An ideal balanced modulator with a source impedance RS and a frequency-dependent load Z_L

The high quality factor can be built by the frequency conversion which can improve the quality factor by changing the operating frequency. In addition, since the filter tuning depends on the switching frequency of the mixer, its tuning range is quite large as long as the switching frequency is available. The inherent image signal due to the signal mixing is removed by the complex mixing principle to automatically generate the opposite phase signal. Section II introduces the principles of the presented frequency conversion structure to build wide tunable high-Q RF filter. The BPF and notch filter are simulated and summarized in Section III. The conclusions are shown in Section IV.

II. Complex Mixing Technique

The basic concept of the frequency conversion structure can start with the typical balanced modulator circuits as shown in Fig. 1. For a frequency-dependent load impedance Z_L, the input impedance Z_{in} is given

$$Z_{in}(\omega) = \frac{4}{\pi^2} \sum_{n=1,3,5\ldots}^{\infty} \frac{1}{n^2} \Big[Z_L(n\omega_{SW} + \omega) + Z_L^*(n\omega_{SW} - \omega) \Big], \tag{1}$$

where ω_{SW} denotes the frequency of a switching signal. Equation (1) shows that the frequency dependent load is modulated with the mixer, and so its frequency response is translated around the switching frequency. However, there should be finite source impedance in the typical RF environment. Moreover, the simple balanced modulator, shown in Fig. 1, does not have an ability to distinguish the desired signal from the image signals. The image signal response of the balanced modulator is illustrated in Fig. 2. If a jammer at ω_J is present at the input along with the desired signal at ω_S, then the image component of the jammer will be translated to ω_S if $2\omega_{SW} - \omega_J = \omega_S$. In this case, if the jammer is significantly larger than the desired signal, it will degrade the signal-to-noise-and-interference ratio (SNIR) of the desired signal.

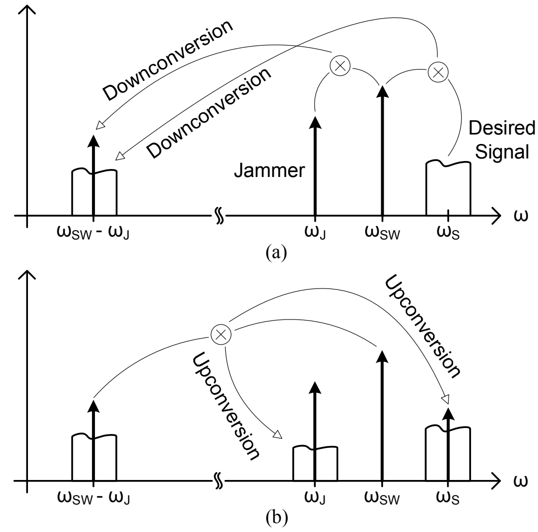

Fig. 2 (a) Downconversion of the desired signal and jammer to baseband, (b) Upconversion of the downconverted desired signal and jammer. Note that the image response of the mixer causes the jammer to appear at the same frequency as the desired signal

This difficulty can be mitigated by the use of an complex passive mixer, which will inherently reject the image signal, as shown in Fig. 3. The input impedance of Fig. 3, $Z_{in\text{-}IQ}$, is given by

$$Z_{in-IQ}(\omega) = \frac{4}{\pi^2} \sum_{n=1,3,5\ldots}^{\infty} \frac{1}{n^2} \left[\left(\frac{R_{eq} Z_L (n\omega_{SW} + \omega)}{R_{eq} + Z_L (n\omega_{SW} + \omega)} \right) + \left(\frac{R_{eq} Z_L (n\omega_{SW} - \omega)}{R_{eq} + Z_L (n\omega_{SW} - \omega)} \right)^* \right], \quad (2)$$

where R_{eq} denotes the equivalent source impedance at the input of each in-phase and quadrature phase path, i.e., $R_{eq} = 2R_S$. To complete the initial design, the on-resistance of the transistor switch, $R_{SW(ON)}$, can be included in the calculation of (2) by replacing $Z_L(n\omega_{SW} \pm \omega)$ with $R_{SW(ON)} + Z_L(n\omega_{SW} \pm \omega)$. Equation (2) is valid for a imaginary load impedance as well.

The image rejection property of the complex passive mixer in Fig. 3 is illustrated in Fig. 4. Since the desired and image signal frequencies are merged after downconversion in the complex passive mixer, there is no signal degradation due to the image signal. An added complication is that the image reject mixer has to maintain near-perfect isolation between in-phase and quadrature phase paths, which is difficult to achieve with a passive mixer when employing a 50 % duty cycle switching signal. Therefore, a 25 % duty cycle switching signal is employed to maintain isolation between in-phase and quadrature phase paths [9].

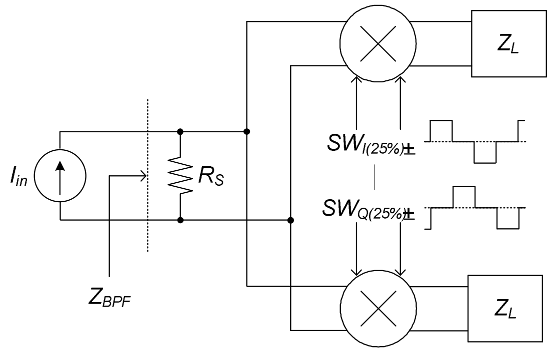

Fig. 3 A tunable impedance $Z_{in\text{-}IQ}$ with image cancellation

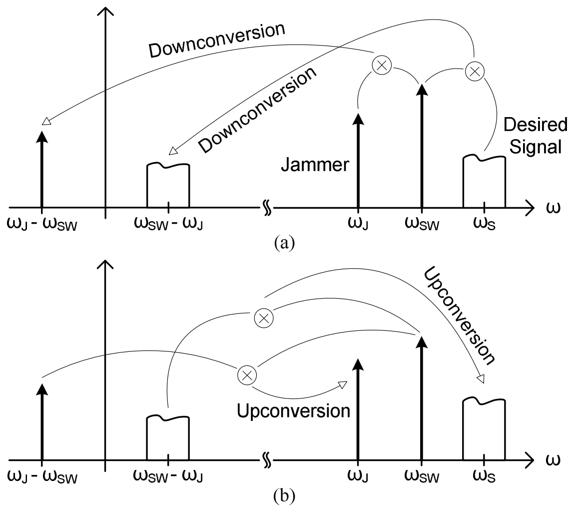

Fig. 4 (a) Complex downconversion of the desired signal and jammer to baseband, (b) Complex upconversion of the downconverted desired signal and jammer

Two different types of RF filters are implemented to verify the frequency conversion based filters shown in Fig. 3. In order to build the RF band-pass filter (BPF), the capacitive termination is used for the frequency dependent load, Z_L, in Fig. 3. For an RF notch filter, the parallel LC tank is used the frequency dependent load.

III. RF Filter Performances

The presented RF filters is quite useful in co-existing multi-standards wireless communications environment. One of those frequency bands is the TV bands. Especially, there is a promising wireless system called cognitive radio (CR), which is proposed to solve the frequency crowding issues by managing the frequency allocation effectively [10]. IEEE 802.22 working group has been developing a world-wide CR-based standard for wireless regional area networks (WRANs) using TV broadcasting service bands [11]. The U.S. Federal Communications Commission (FCC) released its order allowing personal portable devices to operate on unoccupied TV channels between 21 and 51, except 37, for IEEE 802.22 applications [12]. These frequencies may be extended to 41 ~ 910 MHz to meet international regulations [13]. In addition, the standard bandwidth of international TV channels varies from 6 to 8 MHz [13]. The presented RF band-pass filter can effectively select the desired frequency band. Fig. 5 shows the frequency response of the BPF and compares the simulation response with the calculations. The tunable RF band-pass filter translates the high impedance of a load capacitor around DC to a RF frequency tuned by the switching signal, and simultaneously suppresses the image signal through the complex mixer. It is very linear due to the switching action of the transistors, and low noise due to the low losses of the CMOS switches.

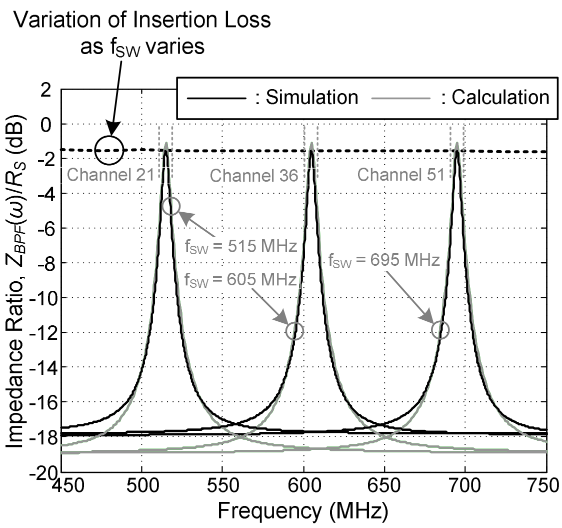

Fig. 5 Comparison of simulated and calculated impedance ratios for the tunable RF band-pass filter. The switching frequencies of 515, 605, and 695 MHz are used. The dashed line at the bottom illustrates the variation of the peak attenuation as the switching frequency varies

TABLE I
PERFORMANCES OF THE TUNABLE RF BAND-PASS FILTER

Design Parameters		Filter Performance	
NMOS	300um/0.1um	Max. Attenuation	18dB
R_S	50Ω	Min. Insertion Loss	1.8dB
C_L	10pF	3dB Bandwidth	5.5MHz
L_L	2uH	Noise Figure	1.7dB

The simulated filter response shows excellent agreement with the calculated response for the switching frequencies of 515, 605, and 695 MHz corresponding to TV channels 21, 36, and 51. The switches in the balanced passive mixers are implemented with NMOS transistors in a 90 nm CMOS technology, with an estimated 2.3 Ω switch on-resistance. The dashed line at the bottom of Fig. 5 illustrates the variation of the peak attenuation as the switching frequency varies. The design parameters and filter performance of the tunable RF band-pass filter are summarized in Table I.

The frequency responses of the tunable RF notch filter are shown and compared with the calculations are shown in Fig. 6, and the design parameters and filter performance of the tunable RF band-pass filter are summarized in Table II.

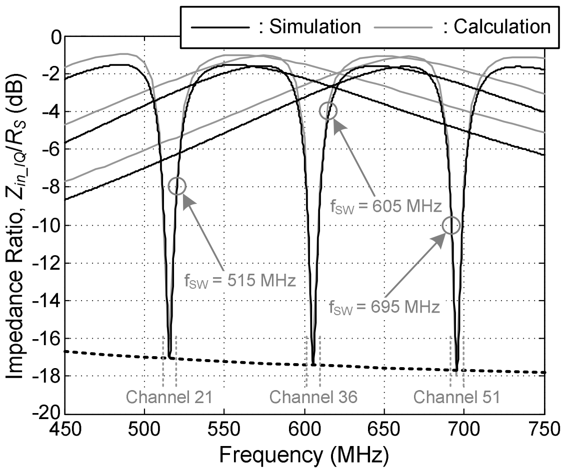

Fig. 6 Comparison of simulated and calculated impedance ratios for the tunable notch filter. The switching frequencies of 515, 605, and 695 MHz are used. The dashed line at the bottom illustrates the variation of the peak attenuation as the switching frequency varies

TABLE II
PERFORMANCES OF THE TUNABLE RF NOTCH FILTER

Design Parameters		Filter Performance	
NMOS	300um/0.1um	Max. Attenuation	17dB
R_S	50Ω	Min. Insertion Loss	1.6dB
C_L	530pF	Quality Factor	32
·	·	Noise Figure	1.7dB

Especially, this notch filter can be useful when there is a nearby known interference. Since the filter must be tunable over a wide frequency range, because the channel allocation of the TV signal will depend on the geographic location of the CR device, and is outside of the control of the CR network. Due to the coexistence with commercial systems, the CR device will receive strong interference signals.

Even though the CR device operates on an empty TV channel, adjacent channel TV signals can interact with the front-end RF devices of the CR device, and produce an in-band interference or DC offset problems possibly critical for the CR receiver performance. A captured TV signal transmitted by a nearby TV station can be as high as -8 dBm [14]. However, the minimum detectable desired CR signal level can be as weak as -102 dBm [14]. Therefore, it puts a heavy burden on the receiver design to process a weak desired signal simultaneously with a strong TV signal. In order to suppress those strong nearby interference at known frequency bands, the presented RF notch filter can be very useful and placed between low noise amplifier (LNA) and RF-mixer in the receiver path, as shown in Fig. 7. At the same time, this technique must have very low loss and distortion.

Generally, the front-end LNA is linear enough. However, the following RF mixer does not show good linearity. The inserted notch filter can relax the dynamic range requirement of the following RF blocks by attenuating the strong interference. In case the front-end have poor linearity to process strong interferences, the proposed RF notch filter can be placed in front of the LNA to relax the linearity requirement of the LNA. However, the overall noise figure (NF) will increase by the amount of the insertion loss of the front-end tunable RF notch filter.

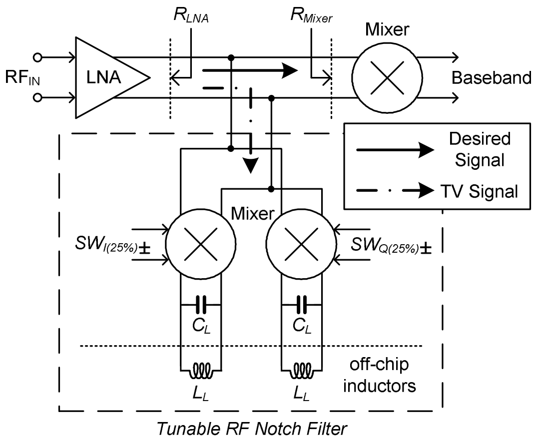

Fig. 7 Realization of a tunable RF notch filter with wide and fine frequency tuning abilities

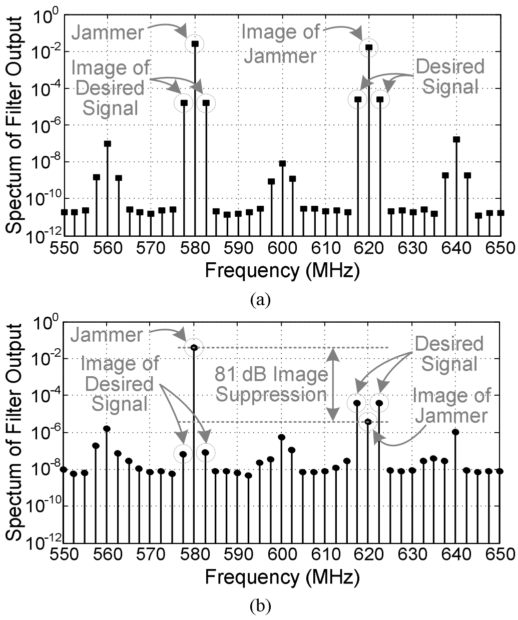

Fig. 8 (a) Spectrum of filter output without image cancellation, (b) Spectrum of filter output with image cancellation. Note that the frequencies of the jammer and switching signal are 580 and 600 MHz, respectively. The desired signal is a two-tone signal at 617.5 and 625.5 MHz

In Fig. 8, the effect of image cancellation is verified by comparing the spectrum of filter output voltage across the source impedance in Fig. 1 using a LC tank load with the load impedance in Fig. 3.

IV. Conclusion

It is shown that the frequency conversion technique is very effective to create the high-*Q* RF filter. The RF band-pass filter (BPF) and notch filter show 1.8dB and 1.6dB insertion losses and 18 dB and 17 dB attenuations, respectively. The quality factor show greater than 30. Even though the insertion loss is limited by the on resistance of the switches, it can be further reduced by additional techniques such as the gate voltage boosting technique. The wide tunable abilities of the presented frequency conversion based RF filters are quite useful property. The presented RF band-pass filter can be very useful in direct channel selection in very crowded frequency bands to remove interference problems. The presented RF filters will have a wide range of potential applications where a single interfering signal must be suppressed, without compromising the SNIR of a nearby desired signal.

Acknowledgment

The authors would like to acknowledge the support of the Korea Electronics Technology Institute (KETI), and notify that this work is founded by Ministry of Science, ICT, and Future Planning.

References

[1] W. D. Yan and R. R. Mansour, "Tunable dielectric resonator bandpass filter with embedded MEMS tuning elements," *IEEE Trans. Microw. Theory Tech.*, vol. 55, no. 1, pp. 154–160, Jan. 2007.

[2] I. Reines, A. Brown, M. El-Tanani, A. Grichener, and G. Rebeiz, "1.6–2.4 GHz RF MEMS tunable 3-pole suspended combline filter," in *Proc.IEEE MTT-S International Microwave Symposium Digest*, 15–20 June 2008, pp. 133–136.

[3] N. Shigekawa, K. Nishimura, T. Suemitsu, H. Yokoyama, and K. Hohkawa, "SAW filters composed of interdigital schottky and ohmic contacts on AlGaN/GaN heterostructures," *IEEE Electron Device Lett.*, vol. 28, no. 2, pp. 90–92, Feb. 2007.

[4] F. Shiba, M. Yamazaki, O. Iijima, and H. Yatsuda, "GPS SAW filter using a wafer level technique," in *Proc. IEEE Ultrasonics Symposium*, 28–31 Oct. 2007, pp. 937–940.

[5] A. Yoshizawa and Y. Tsividis, "A channel-select filter with agile blocker detection and adaptive power dissipation," *IEEE J. Solid-State Circuits*, vol. 42, no. 5, pp. 1090–1099, May 2007.

[6] Y. Palaskas and Y. Tsividis, "Power-area-DR-frequency-selectivity tradeoffs in weakly nonlinear active filters," in *Proc. International Symposium on Circuits and Systems ISCAS '03*, vol. 1, 25–28 May 2003, pp. I–453–I–456.

[7] A. Yoshizawa and Y. Tsividis, "A channel-select filter with agile blocker detection and adaptive power dissipation," *IEEE J. Solid-State Circuits*, vol. 42, no. 5, pp. 1090–1099, May 2007.

[8] Y. Palaskas and Y. Tsividis, "Power-area-DR-frequency-selectivity tradeoffs in weakly nonlinear active filters," in *Proc. International Symposium on Circuits and Systems ISCAS '03*, vol. 1, 25–28 May 2003, pp. I–453–I–456.

[9] H. Khatri, L. Liu, T. Chang, P. S. Gudem, and L. E. Larson, "A SAW-less CDMA receiver front-end with single-ended LNA and single-balanced mixer with 25% duty-cycle LO in 65nm CMOS," in *Proc. IEEE Radio Frequency Integrated Circuits Symposium RFIC 2009*, 7–9 June 2009, pp. 13–16.

[10] J. Mitola III, "Cognitive radio for flexible mobile multimedia communications," in *Proc. IEEE International Workshop on Mobile Multimedia Communications*, 15-17 Nov. 1999, pp. 3-10.
[11] IEEE 802.22 Working Group, http://www.ieee802.org/ 22/.
[12] FCC, "In the matter of unlicensed operation in the TV broadcast bands: second report and order and memorandum opinion and order," Tech. Rep. 08-260, Nov. 14 2008.
[13] S. Haykin, "Cognitive radio: brain-empowered wireless communications," *IEEE J. Sel. Areas Commun.*, vol. 23, no. 2, pp. 201–220, Feb 2005.
[14] E. Au, G. Chouinard, and Z. Lei, "IEEE P802.22 wireless RANs receiver performance evaluation criteria," IEEE 802.22-08/0326r2, http://www.ieee802. org/22/, Dec. 2008.